Supplementary data for the article:

Poljarević, J. M.; Tamás Gál, G.; May, N. V.; Spengler, G.; Dömötör, O.; Savić, A. R.; Grgurić-Šipka, S.; Enyedy, É. A. Comparative Solution Equilibrium and Structural Studies of Half-Sandwich Ruthenium(II)(η 6 -Toluene) Complexes of Picolinate Derivatives. *J. Inorg. Biochem.* **2018**, *181*, 74–85. https://doi.org/10.1016/j.jinorgbio.2017.12.017

SUPPLEMENTARY INFORMATION

Comparative solution equilibrium and structural studies of half-sandwich ruthenium(II)(η^6-toluene) complexes of picolinate derivatives

Jelena M. Poljarević, G. Tamás Gál, Nóra V. May, Gabriella Spengler, Orsolya Dömötör, Aleksandar R. Savić, Sanja Grgurić-Šipka, Éva A. Enyedy*

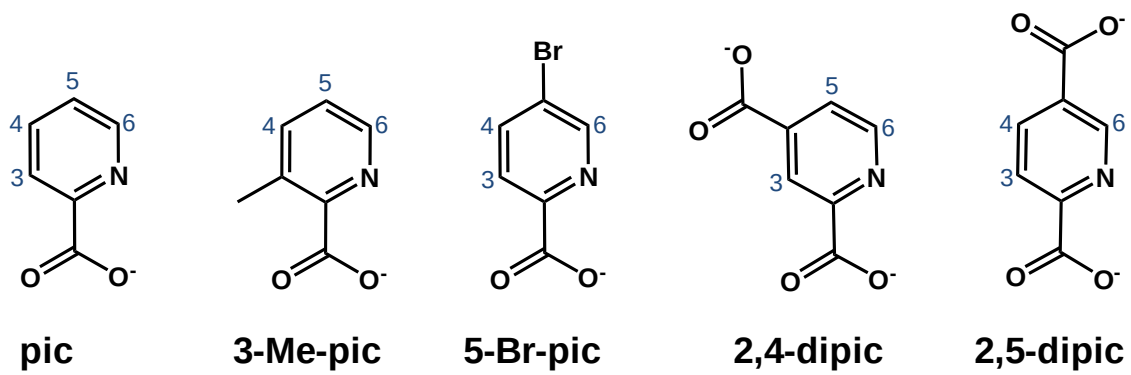

Chart S1. Chemical structures of the ligands in their completely deprotonated forms with numbering of the ring protons.

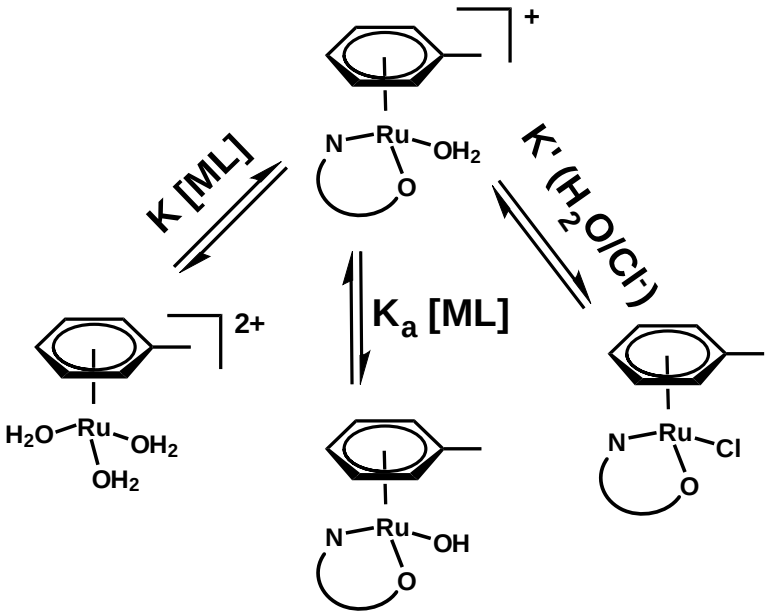

Chart S2. Complexation and co-ligand exchange equilibrium processes for the [Ru(η^6-toluene (L)(H_2O)]$^+$ species.

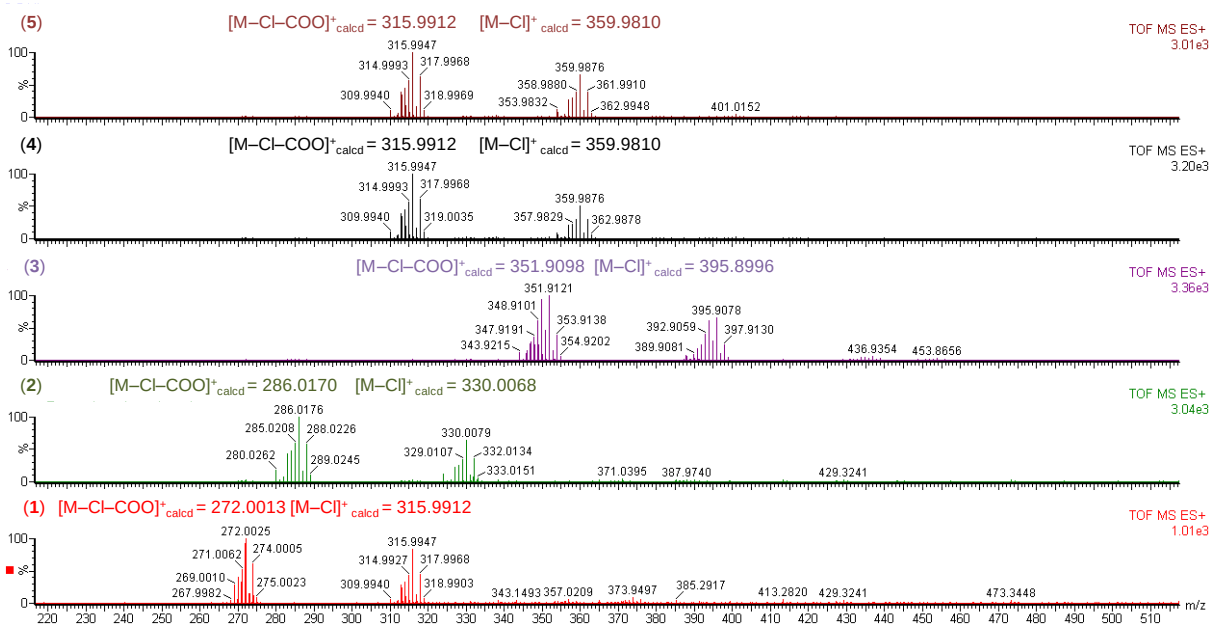

Figure S1. ESI-MS spectra of complexes **1**-**5** with the theoretical values.

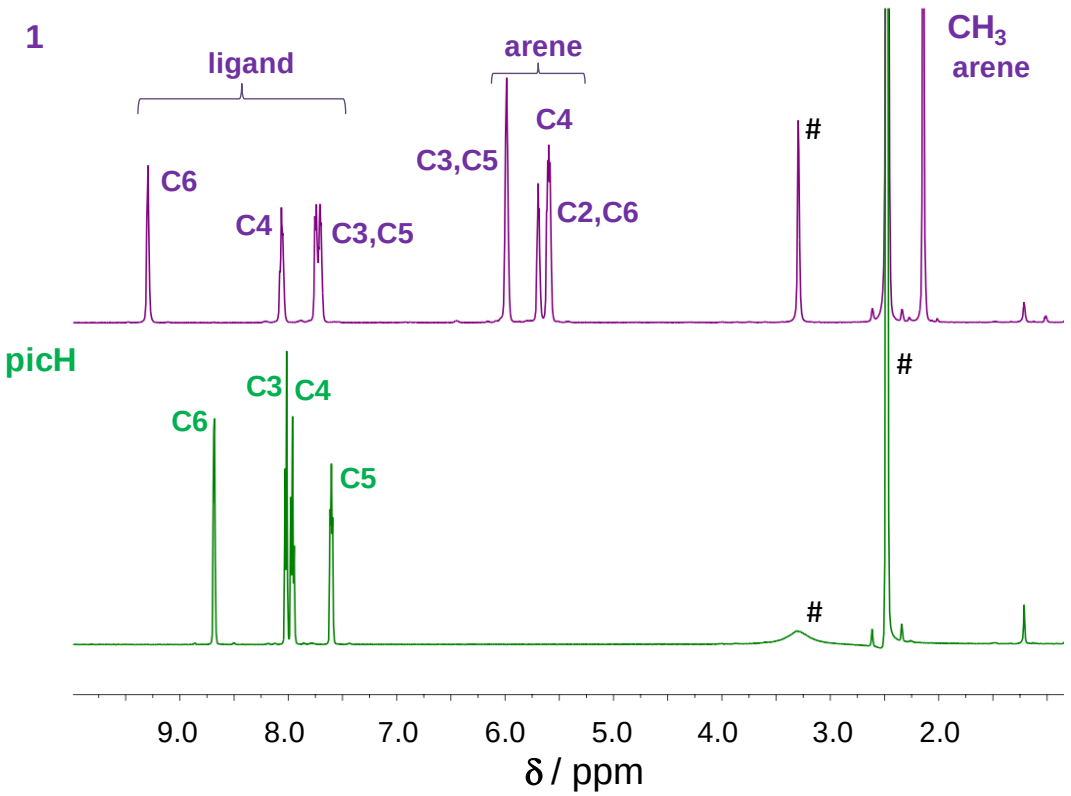

Figure S2. ^{1}H NMR spectra of complex **1** and ligand picH in DMSO-d_6 (solvent peaks: #).

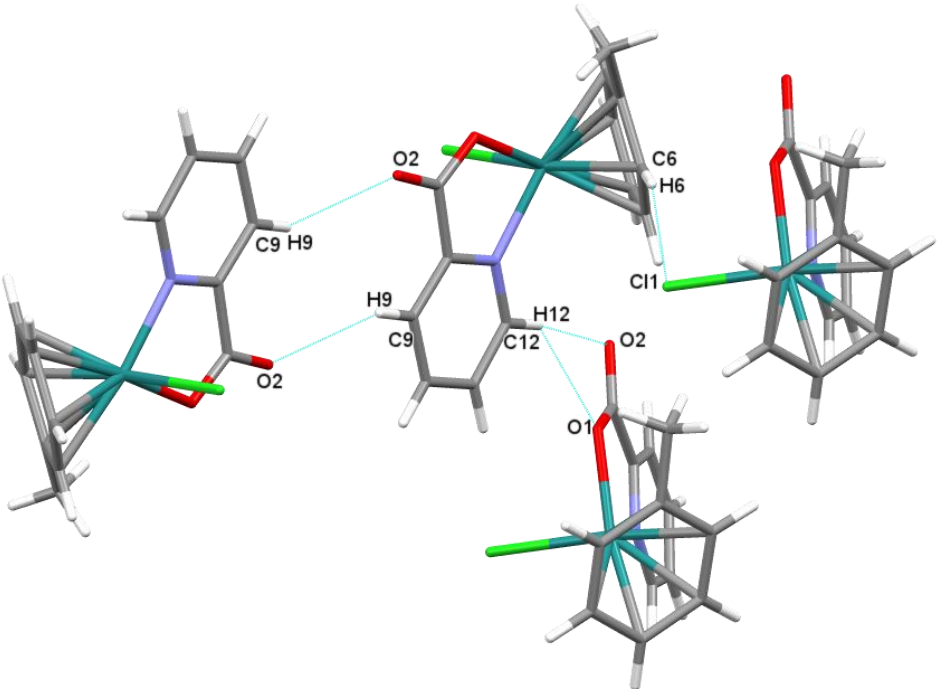

Figure S3. Packing arrangement showing the system of the hydrogen bonds in crystal **1**. Details of hydrogen bond parameters are collected in Table S2.

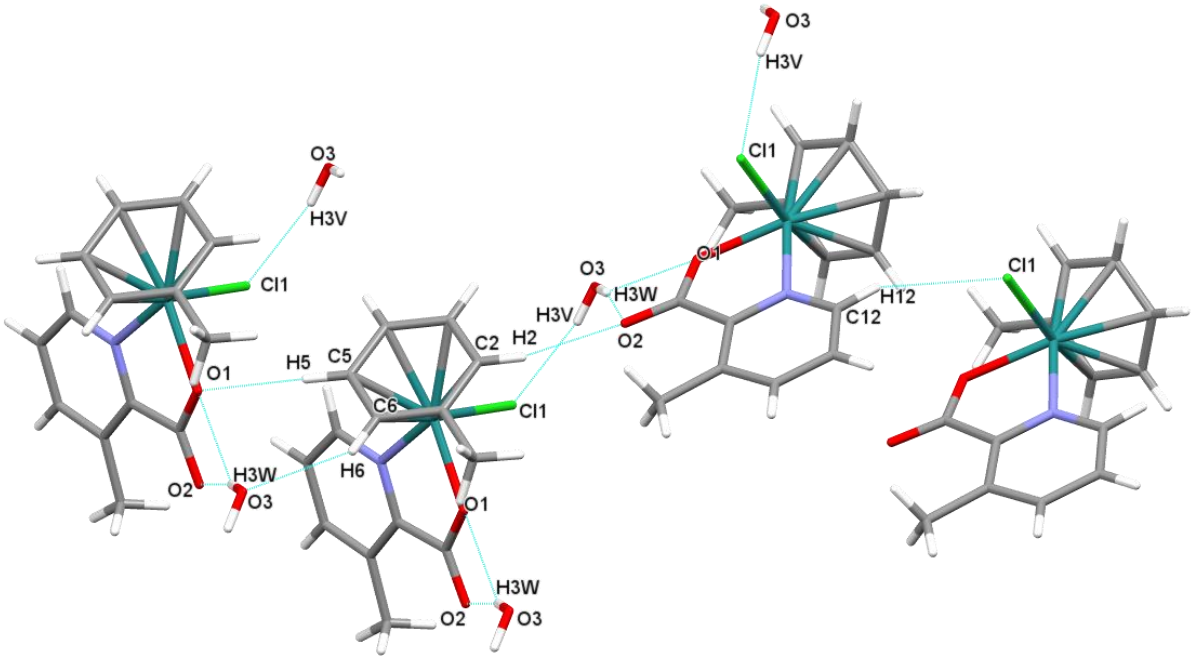

Figure S4. Packing arrangement showing the system of the hydrogen bonds in crystal **2**·H_2O. Details of hydrogen bond parameters are collected in Table S2.

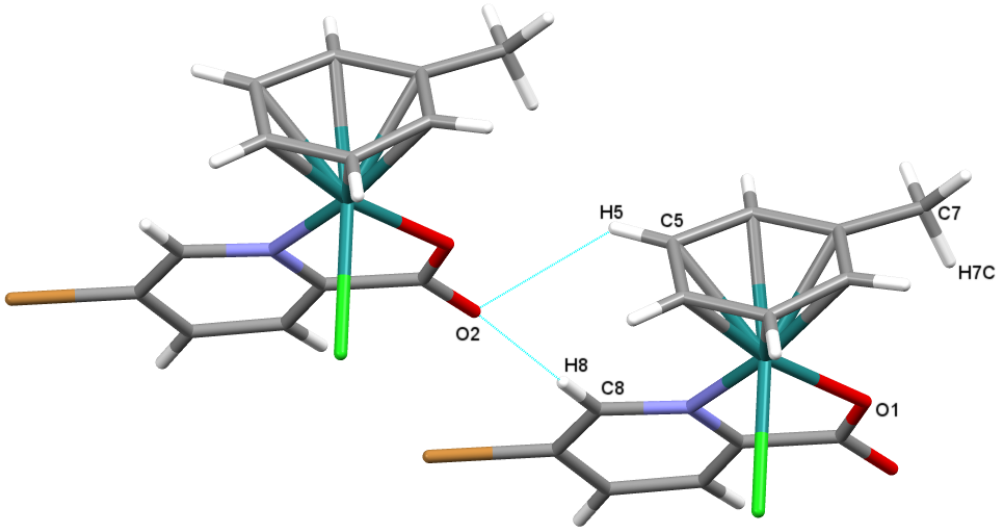

Figure S5. Packing arrangement showing the system of the hydrogen bonds in crystal **3**. Details of hydrogen bond parameters are collected in Table S2.

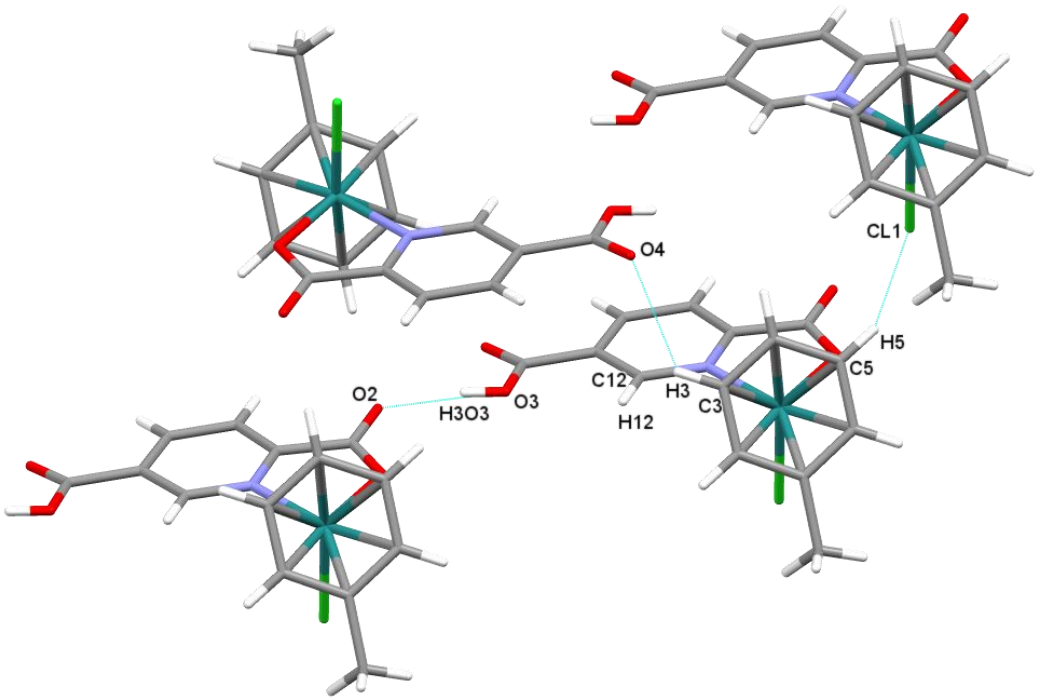

Figure S6. Packing arrangement showing the system of the hydrogen bonds in crystal **4**. Details of hydrogen bond parameters are collected in Table S2.

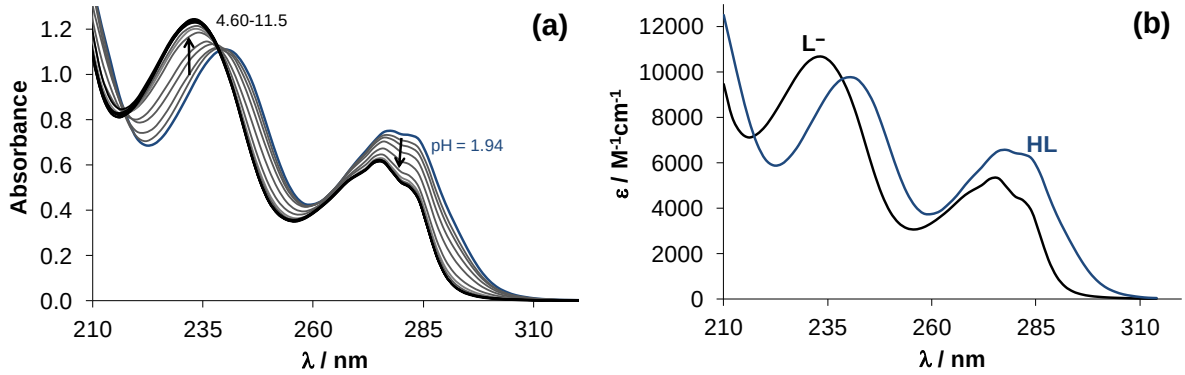

Figure S7. UV-vis spectra of 5-Br-picH recorded at various pH values (a), calculated individual absorption spectra of ligand species (b). {$c_{5\text{-}Br\text{-}pic}$ = 115 μM; pH = 2 – 11.5; T = 25 °C; I = 0.20 M (KCl); ℓ = 1.0 cm}

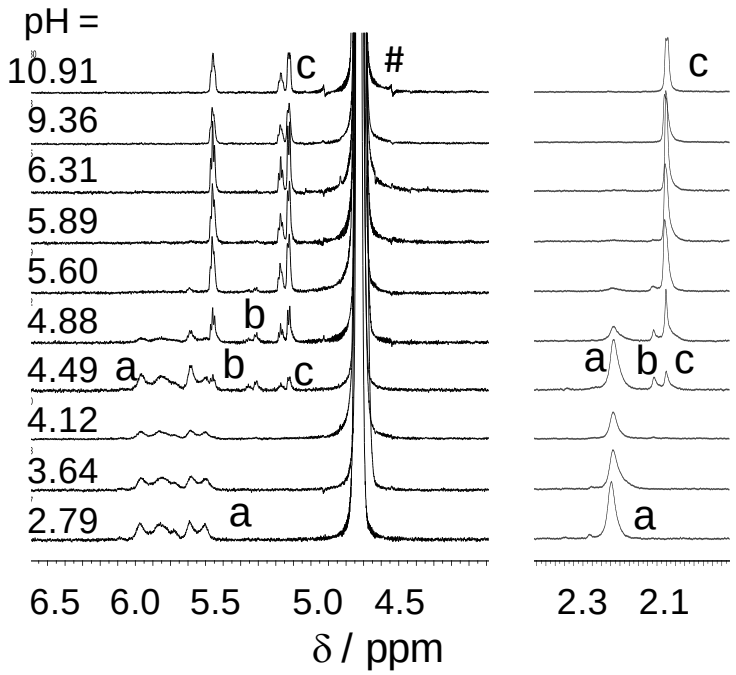

Figure S8. ^{1}H NMR spectra of [Ru(η^6-toluene)(Z)$_3$] (Z = Cl^-/H_2O) in aqueous solution in the presence of 0.20 M chloride ion at the indicated pH values in the regions of the toluene CH protons (left side) and the CH_3 protons (right side). Identified species: **a**: [Ru(η^6-toluene)$(H_2O)_2Cl]^+$ (= M); **b**: [(Ru(η^6-toluene))$_2(\mu^2$-OH)$_2Cl]^+$ (= [$M_2(OH)_2$]); **c**: [(Ru(η^6-toluene))$_2(\mu^2$-OH)$_3]^+$ (= [$M_2(OH)_3$]); #: solvent peak. {c_{Ru} = 1 mM; T = 25 °C; I = 0.20 M (KCl); D_2O; pH = pD×0.93+0.40 [55]}

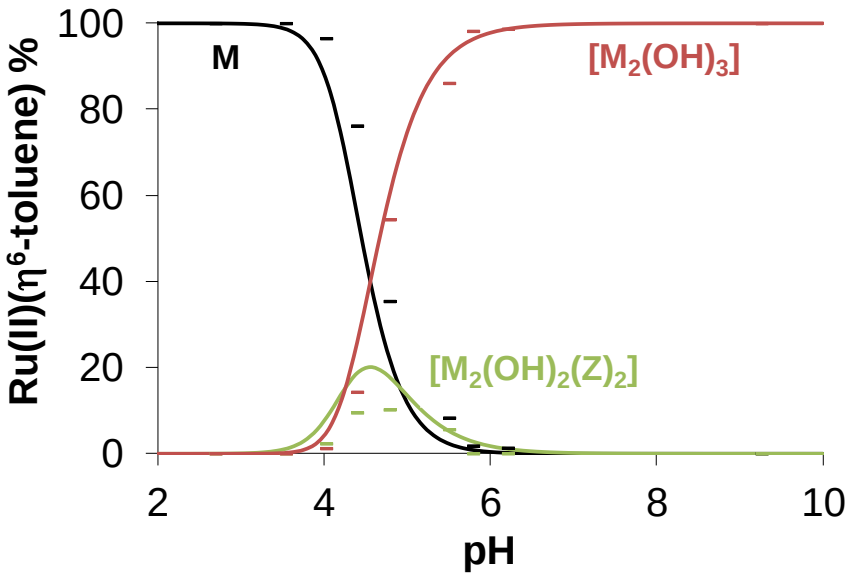

Figure S9. Concentration distribution curves for [Ru(η^6-toluene)$(Z)_3$] (where Z = H_2O/Cl^-) in aqueous solution in the presence of 0.20 M chloride ions in the pH range from 2 up to 10 together with the ^{1}H NMR peak integrals for the CH_3 toluene protons of M, $[M_2(OH)_2]$ and $[M_2(OH)_3]$ species identified based on Fig. S8. {c_{Ru} = *1 mM; T = 25 ˚C; I = 0.20 M (KCl)*}

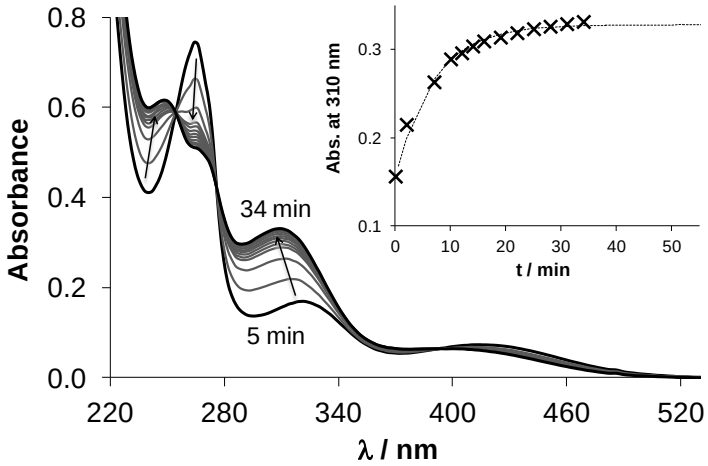

Figure S10. Time-dependence of UV-vis absorption spectra recorded for the [Ru(η^6-toluene)$(H_2O)_3$]$^{2+}$ – picH (1:1) system at pH = 2.79 in the presence of chloride ions. The inset shows the absorbance changes at 310 nm. {c_{Ru} = c_L = *102 μM; T = 25 ˚C; I = 0.20 M (KCl);* ℓ *= 1.0 cm*}

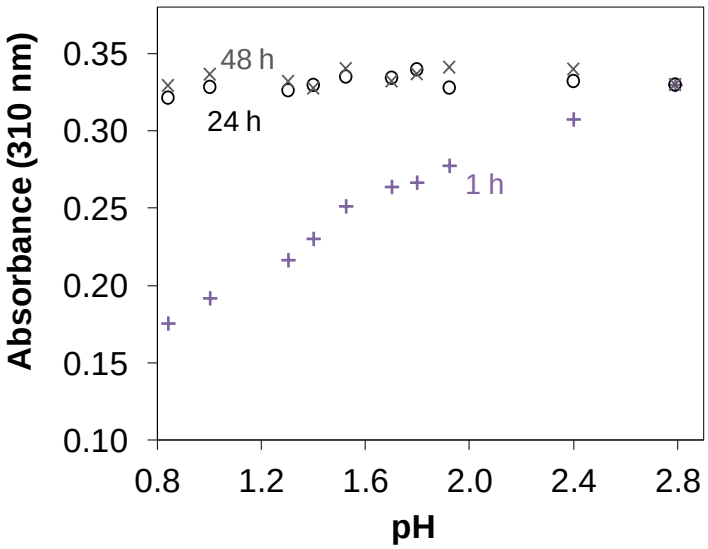

Figure S11. Absorbance values at 310 nm recorded for the $[Ru(\eta^6\text{-toluene})(H_2O)_3]^{2+}$ – picH (1:1) system after 1 h, 24 h and 48 h waiting time in the presence of chloride ions at pH = 0.85 -2.79 using individual samples. {$c_{Ru} = c_L = 102\ \mu M;\ T = 25\ ^{\circ}C;\ I = 0.20\ M\ (KCl);\ \ell = 1.0\ cm$}

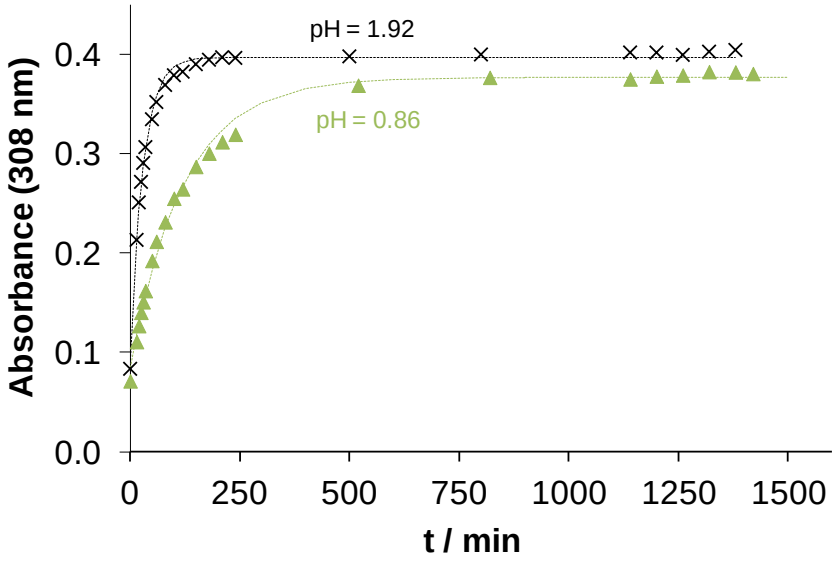

Figure S12. Time-dependence of absorbance values at 308 nm recorded for the $[Ru(\eta^6\text{-toluene})(H_2O)_3]^{2+}$ – 3-Me-picH (1:1) system at pH = 1.92 (×) and at 0.86 (▲) in the presence of chloride ions with the fitted kinetic curves (dashed lines). {$c_{Ru} = c_L = 123\ \mu M;\ T = 25\ ^{\circ}C;\ I = 0.20\ M\ (KCl);\ \ell = 1.0\ cm$}

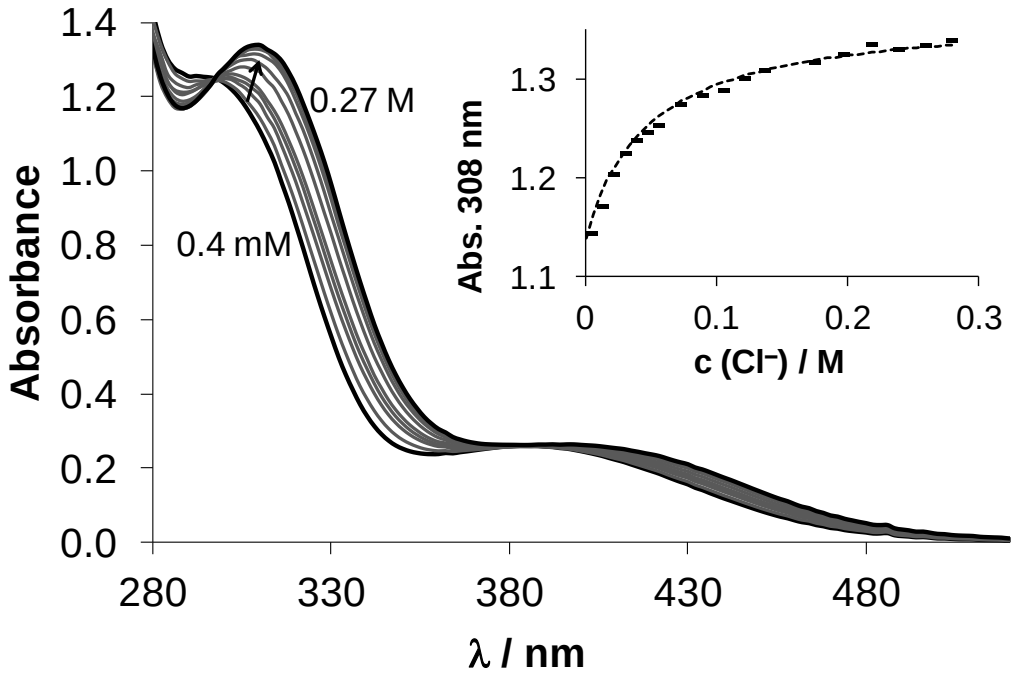

Figure S13. UV-vis spectra recorded for the water/chlorido exchange process in the complex **1** at pH = 5.50. Inset shows measured (−) and fitted absorbance values (dashed line) at 308 nm and at various chloride ion concentrations. {$c_{Ru} = c_L = 0.08$ mM; $c_{Cl^-} = 0$–270 mM; $T = 25$ ˚C}

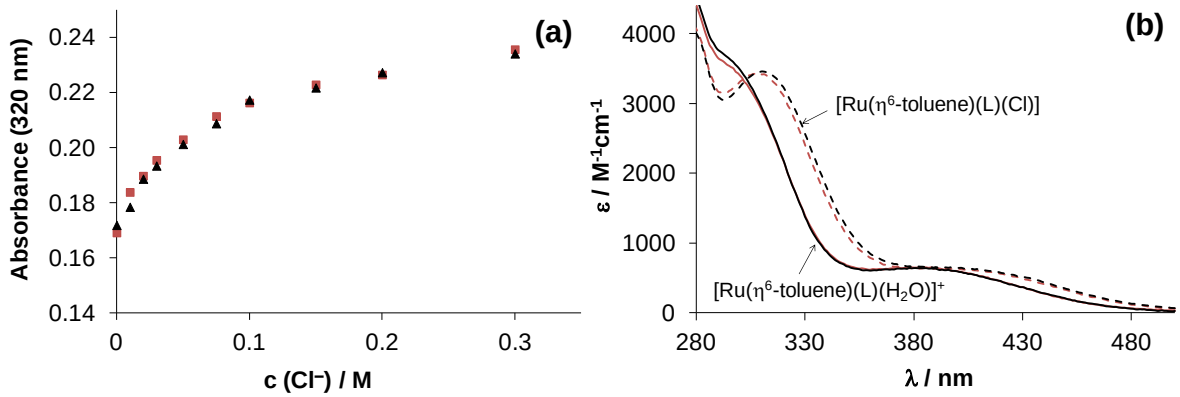

Figure S14. Absorbance values recorded at 320 nm for the water/chlorido exchange process in the complex **2** at pH = 6.70 at variable ionic strength (■) and at a constant ionic strength of 0.30 M $NaClO_4$/NaCl (▲) (a). Calculated molar absorbance spectra for the aqua (solid lines) and chlorido (dashed lines) complexes at variable (red) and constant ionic strength (black) (b). {$c_{Ru} = c_L = 0.08$ mM; $c_{Cl^-} = 0$–300 mM; $T = 25$ ˚C}

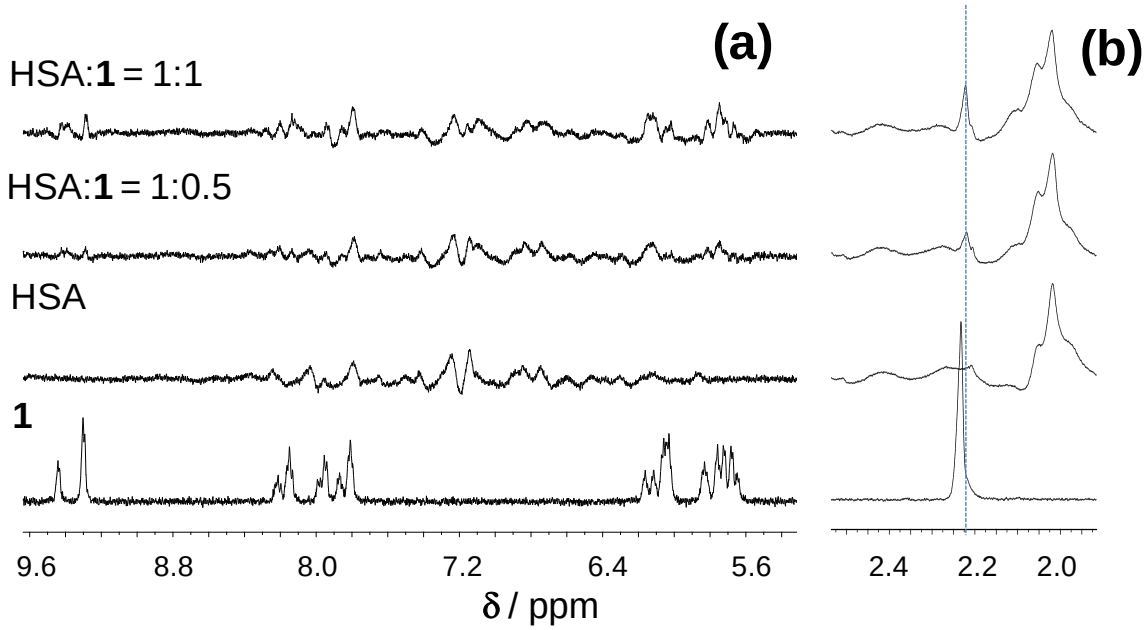

Figure S15. ^{1}H NMR spectra of **1**, HSA and HSA:**1** systems in PBS' buffer at pH 7.4 in the regions of the ligand and toluene CH protons (a) and the CH_3 toluene protons (b). {*c_1 = 1.0 or 0.5 mM; c_{HSA} = 0.5 mM; T = 25 ˚C; 10% D_2O, incubation time: 24 h*}

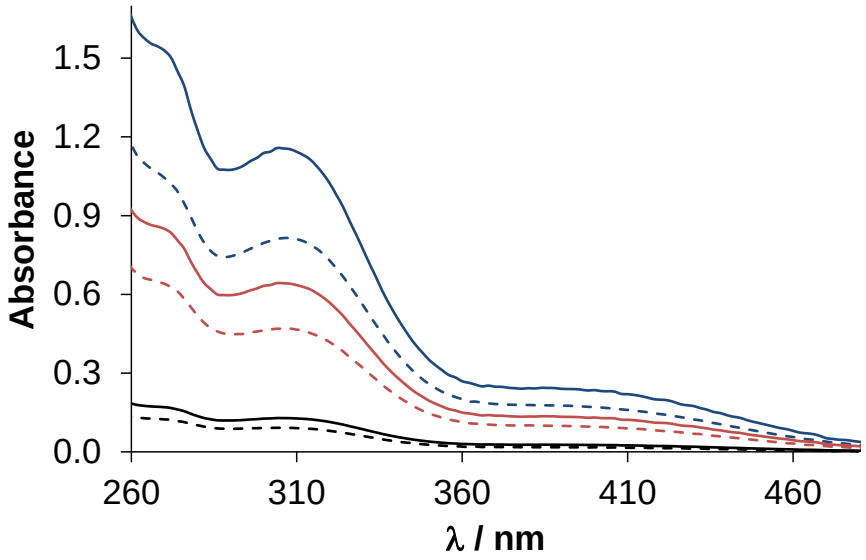

Figure S16. UV-vis spectra recorded for the LMM fractions of the ultrafiltered samples of HSA–**1** (dashed lines) with the corresponding reference spectra of samples containing **1** (solid lines). {*Original sample composition: HSA: 40 μM, or 0 M for the references; **1**: 366 μM (blue); 203 μM (red); 40 μM (black); T = 25 ˚C; pH = 7.4 in PBS'*; *incubation time: 24 h*}

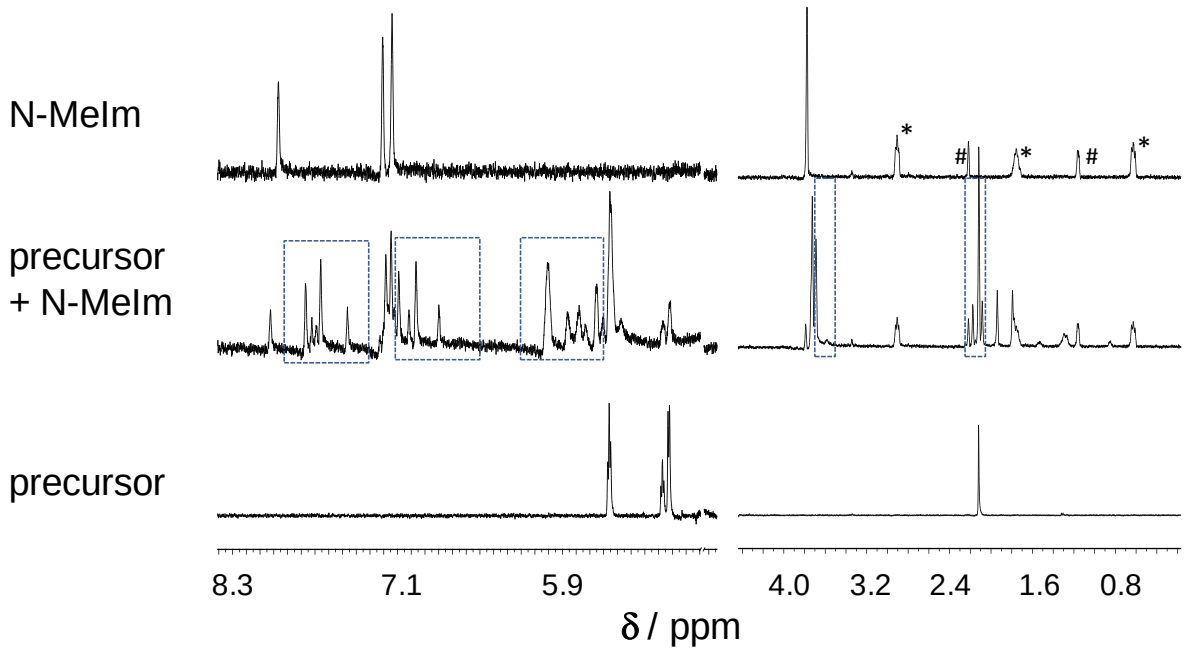

Figure S17. ^{1}H NMR spectra of N-MeIm, the $[Ru(\eta^6\text{-toluene})Cl(\mu\text{-}Cl)]_2$ – N-MeIm (1:1) system and the precursor alone at pH 7.4 in PBS'. The framed details of spectra with dashed line indicate peaks belonging to the $Ru(\eta^6\text{-toluene})$ complexes formed with N-MeIm .{*c = 1 mM; T = 25 °C; 10% D_2O; *: DSS peaks; #: solvent peaks*}

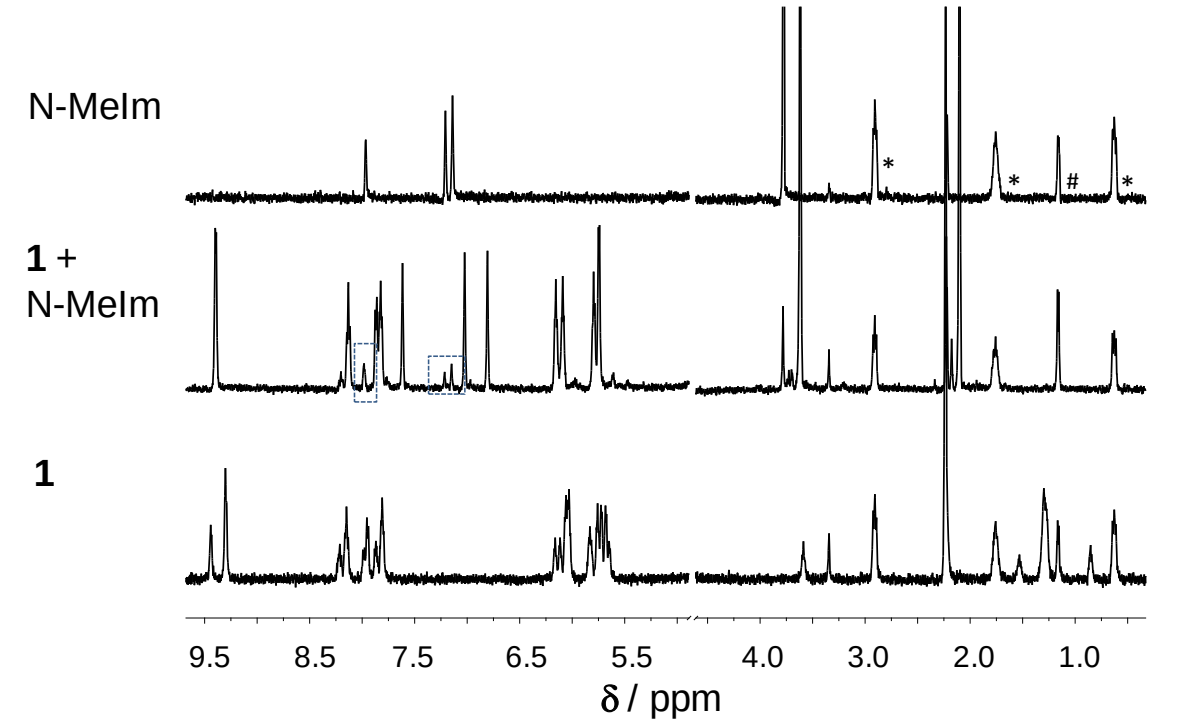

Figure S18. ^{1}H NMR spectra of N-MeIm, the **1** – N-MeIm (1:1) system and **1** alone at pH 7.4 in PBS'. The framed details of spectra with dashed line indicate peaks belonging to the unbound N-MeIm and were used for the calculation of the integrals. {*c = 1 mM; T = 25 °C; 10% D_2O; *: DSS peaks; #: solvent peaks*}

Table S1. Crystal data and structure refinement for complexes **1-3** and **5**

Compound	**1**	**2**·H_2O	**3**	**5**
Color/shape	Orange/Prism	Yellow/Prism	Yellow/Prism	Yellow/Prism
Empirical formula	$C_{13}H_{12}ClNO_2Ru$	$C_{14}H_{16}ClNO_3Ru$	$C_{13}H_{11}ClNO_2Ru$	$C_{14}H_{12}ClNO_4Ru$
Moiety formula	**$[Ru(C_{13}H_{12}NO_2)(Cl)]$**	**$[Ru(C_{14}H_{14}NO_2)(Cl)]\cdot H_2O$**	**$[Ru(C_{13}H_{11}NO_2)(Cl)]$**	**$[Ru(C_{14}H_{12}NO_4)(Cl)]$**
Formula weight (g/mol)	350.76	382.80	429.66	394.77
Temperature (K)	103(2)	103(2)	293(2)	293(2)
Radiation and wavelength λ	Mo-Kα, 0.71075	Mo-Kα, 0.71075	Mo-Kα, 0.71075	Mo-Kα, 0.71075
Crystal system	monoclinic	monoclinic	triclinic	triclinic
Space group	$P\,2_1/n$	$P\,2_1$	P-1	P-1
Unit cell dimensions				
a (Å)	8.2995(3)	6.1442(6)	7.616(3)	7.6948(14)
b (Å)	14.9714(5)	13.7320(14)	7.754(4)	9.6578(19)
c (Å)	10.0795(4)	8.3347(10)	12.938(6)	11.251(2)
α (°)	90	90	81.590(10)	98.060(7)
β (°)	94.1300(10)	91.468(3)	86.380(18)	106.159(7)
γ (°)	90	90	61.66(4)	109.866(8)
Volume ($Å^3$)	1973.30(13)	702.99(13)	665.2(6)	729.3(2)
Z/Z'	4/1	2/1	2/1	2/1
Density (calc.) (Mgm^{-3})	1.865	1.808	2.145	1.798
Absorption coefficient, μ (mm^-	1.460	1.310	4.377	1.271
F(000)	696	384	416	392
Crystal size (mm)	0.50 x 0.25 x 0.25	0.50 x 0.10 x 0.10	0.50 x 0.10 x 0.05	0.25 x 0.10 x 0.05
Absorption correction	numerical	numerical	numerical	numerical
Min. and max. transmission	0.5596 and 0.7490	0.6975 and 0.9496	0.5635 and 0.8517	0.861 and 0.962
θ–range for data collection (°)	$3.073 \le \theta \le 27.448$	$3.317 \le \theta \le 25.331$	$3.011 \le \theta \le 26.372$	$2.977 \le \theta \le 27.420$
Index ranges	$-10 \le h \le 10;-19 \le k \le 19;-13 \le$	$-7 \le h \le 7;-16 \le k \le 16;-10 \le$	$-9 \le h \le 9;-9 \le k \le 9;-16 \le l \le$	$-9 \le h \le 9;-12 \le k \le 12;-14 \le l$
Reflections collected	46142	10100	5157	6875

Completeness to 2θ	0.999	0.998	0.990	0.997
Independent reflections (R_{int})	2849 (0.0332)	2564 (0.0838)	2671 (0.1239)	3290 (0.0960)
Reflections $I>2\sigma(I)$	2817	2355	1654	1927
Refinement method	full-matrix least-squares on	full-matrix least-squares on	full-matrix least-squares on	full-matrix least-squares on
Data / restraints / parameters	2849 /0 /164	2564 /4 /190	2671 /0 /173	3290 /0 /192
Goodness-of-fit on F^2	1.255	1.071	1.084	1.039
Final R indices [$I>2\sigma(I)$] R_1,	0.0214, 0.0583	0.0442, 0.0810	0.0985, 0.2456	0.0939, 0.1435
R indices (all data) R_1, wR_2	0.0217, 0.0585	0.0503, 0.0852	0.1373, 0.3049	0.1685, 0.1678
Max. and mean shift/esd	0.000;0.000	0.000;0.000	0.000;0.000	0.000;0.000
Largest diff. peak and hole	0.994;-0.425	0.851;-0.931	2.057;-2.337	1.264;-0.876

Table S2. Intermolecular interactions in the crystal structures of complexes **1-3** and **5**.

D-H…A	D…H (Å)	H…A (Å)	D…A (Å)	D-H…A (°)
1				
O6-H6…Cl1[i]	0.95	2.69	3.557(2)	153
C9-H9…O2[ii]	0.95	2.42	3.196(2)	138
C12-H12…O1[iii]	0.95	2.38	3.022(2)	124
2·H_2O				
O3-H3v…Cl1[iv]	0.84(6)	2.35(7)	3.182(10)	169(17)
O3-H3w…O1[v]	0.84(6)	2.40(10)	3.047(12)	134(9)
O3-H3w…O2[v]	0.84(6)	2.29(5)	3.120(12)	169(10)
C2-H2…O2[vi]	0.95	2.31	3.246(17)	168
C5-H5…O1[vii]	0.95	2.37	3.318(12)	179
C6-H6…O3[viii]	0.95	2.48	3.244(14)	138
C12-H12…Cl1[vii]	0.95	2.79	3.671(10)	155
3				
C5-H5…O2[ix]	0.93	2.47	3.11(2)	125
C7-H7c…O1 (intra)	0.96	2.46	3.092(18)	124
C8-H8…O2[ix]	0.93	2.33	3.26(2)	177
5				
O3-H3O3…O2[x]	0.82	1.76	2.570(10)	169
C3-H3…O4[xi]	0.93	2.51	3.183(14)	130
C5-H5…Cl1[vii]	0.93	2.83	3.466(15)	127
C12-H12…O3 (intra)	0.93	2.39	2.723(13)	101

Symmetry codes: [i]1/2+x,1/2-y,1/2+z, [ii]1-x,1-y,-z, [iii]-1/2+x,1/2-y,1/2+z, [iv]1-x,1/2+y,1-z, [v]x,y,-1+z, [vi]1-x,-1/2+y,2-z, [vii]1+x,y,z, [viii]1+x,y,1+z, [ix]-1+x,y,z, [x]x,1+y,z, [xi]2-x,1-y,-z

Table S3. *In vitro* antiproliferative and cytotoxic effects: IC_{50} values in μM in two human cancer cell lines (sensitive and multidrug resistant) and normal embryonic lung fibroblasts presented for the complexes **1-5**, the corresponding free ligands, the precursor $[Ru(\eta^6\text{-toluene})Cl(\mu\text{-}Cl)]_2$ and cisplatin as well as the for comparison.

	Antiproliferative effect (μM)		**Cytotoxic effect (μM)**		
	Colo 205 sensitive	**Colo 320 resistant**	**Colo 205 sensitive**	**Colo 320 resistant**	**MRC-5 normal** embryonic lung fibroblasts
1	>100	84.84 ± 4.79	>100	>100	>100
2	>100	79.19 ± 6.71	>100	>100	>100
3	>100	>100	>100	>100	>100
4	>100	>100	>100	>100	>100
5	>100	>100	>100	>100	>100
picH	>100	>100	>100	>100	>100
3-Me-picH	>100	>100	>100	>100	>100
5-Br-picH	>100	>100	>100	>100	>100
2,4-dipicH_2	>100	>100	>100	>100	>100
2,5-dipicH_2	>100	>100	>100	>100	>100
Ru precursor	>100	>100	>100	>100	>100
cisplatin	23.2 ± 2.95	2.33 ± 0.04	63.82 ± 4.06	16.06 ± 4.06	33.45± 5.12

Table S4. pK_a of the complexes $[ML(H_2O)]^+$ in the absence of chloride ions, the estimated Cl^-/H_2O exchange constants (log*K*' (H_2O/Cl^-) for the $[ML(H_2O)]^+ + Cl^- \rightleftharpoons [ML(Cl)] + H_2O$ equilibrium, estimated ratio of the chlorinated complex [ML(Cl)] at 100 and 4 mM chloride ion concentrations, and representative IC_{50} values measured in human cancer cells for the complexes of [Ru(η^6-toluene)(pic)Cl] (**1**), [Ru(η^6-*p*-cymene)(pic)Cl], [Os(η^6-*p*-cymene)(pic)Cl] and [Rh(η^5-C_5Me_5)(pic)Cl].

	1	[**Ru**(η^6-*p*-cymene)(pic)Cl]	[**Os**(η^6-*p*-cymene)(pic)Cl]	[**Rh**(η^5-C_5Me_5)(pic)Cl]
p*K*$_a$ (0 M Cl^-)	7.87	8.00 [b]	6.67 [e]	9.32 [f]
log*K*' (H_2O/Cl^-)	1.3 ±0.1	1.4 ± 0.1 [c]	n.d.	2.20 [f]
rate of Cl^-/H_2O	fast	fast [b]	slower [e] $t_{1/2}$ ~ 12 min	fast [f]
[ML(Cl)] fraction				
c(Cl^-) = 100 mM	68%	87% [b]	100% [e]	94% [f]
c(Cl^-) = 4 mM	8%	22% [b]	28% [e]	36% [f]
IC_{50} (μM)	>100 (Colo205) [a]	82 (HeLa) [d] 36 (FemX) [d]	17 (A549) [e] 4.5 (A2780) [e]	343 (A549) [f] 258 (CH1) [f]

[a] Antiproliferative activity: 84.84 mM in Colo320. [b] Data taken from Ref. 23. [c] log*K*' = 1.83 reported in Ref. 23 determined by ^{1}H NMR spectroscopy was revised and a new data was determined by UV-vis spectrophotometry. [d] Data taken from Ref. 27. [e] Data taken from Ref. 29. [f] Data taken from Ref. 56.